

Intelligent Power Management Control for Hybrid Wind Solar Battery Systems Connected to Micro-Grids



Yousra Izgheche^{1*}, Tahar Bahi², Amira Lakhdera²

¹ Department of Electronic, Laboratory of Automatic and Signal Annaba, Annaba 23000, Algeria

² Department of Electrotechnic, Laboratory of Automatic and Signal Annaba, Annaba 23000, Algeria

Corresponding Author Email: yousra.izgheche@univ-annaba.dz

Copyright: ©2024 The authors. This article is published by IETA and is licensed under the CC BY 4.0 license (<http://creativecommons.org/licenses/by/4.0/>).

<https://doi.org/10.18280/jesa.570429>

ABSTRACT

Received: 28 June 2024

Revised: 2 August 2024

Accepted: 14 August 2024

Available online: 27 August 2024

Keywords:

optimization, hybrid system, energy storage, battery, management, SOC, FLC

The use of renewable energy presents a viable alternative to fossil fuels. However, their intermittent nature does not allow for an immediate response to energy demand. Thus, it is necessary and beneficial to harness various renewable sources and integrate a storage system as an auxiliary source to mitigate this intermittency. The hybridization of energy sources requires efficient management of power flows to ensure the proper functioning of the overall system, regardless of changing weather conditions. In this paper, we propose an intelligent power management control for hybrid wind-solar-battery systems connected to micro-grids based on fuzzy logic. The proposed control approach addresses several specific challenges compared to conventional methods in the intelligent energy management of renewable hybrid systems. It effectively manages the uncertainties and nonlinearities inherent in weather variations, optimizes performance by dynamically adjusting the operations of energy sources and storage systems, and ensures efficient real-time utilization of available energy resources, thus providing greater flexibility and adaptability. Additionally, it enhances the stability and reliability of micro-grids by integrating more flexible and adaptive decision-making mechanisms. The simulation results using MatLab/Simulink demonstrate the significant advantage of this intelligent management lies in its ability to precisely control the state of charge of the battery across five distinct levels, which is not achievable using traditional management practices that rely solely on the maximum and minimum levels of the state of charge.

1. INTRODUCTION

The growing development of renewable energies, notably photovoltaic and wind power, brings undeniable advantages both economically and environmentally, thus promoting the transition towards cleaner and more sustainable energy. However, the isolated use of these sources significantly limits their benefits and performance [1]. It is in this context that the hybridization of renewable sources, grouped within a multi-source system called a hybrid system, emerges as a solution [2]. This approach aims to ensure a stable and uninterrupted power supply, meeting the required energy needs.

Hybrid systems [3], which combine renewable sources such as photovoltaic generators (PVG), wind turbines (WT) with batteries as energy storage systems (ESS), and are connected to the electrical distribution grid [4], are specifically designed to provide the necessary power to the load, regardless of meteorological fluctuations and variations in the availability of individual sources [5]. Furthermore, the common use of an energy storage system (ESS) is observed in standalone applications [6]. Renewable energy hybrid systems require various control techniques to ensure efficient energy transfer, requiring considerable technical attention and generating research in this field [7]. Simulations have been conducted on a hybrid energy system to evaluate state of charge (SOC)

control under different load demand scenarios and weather conditions [8]. In parallel, solar and wind are identified as clean and renewable energy sources. Photovoltaic systems face challenges due to the nonlinear properties of solar radiation, while the variability of wind speed makes obtaining constant energy from wind power complex [9]. The integration of artificial intelligence techniques in energy harvesting is being explored to improve performance, quality, and speed compared to conventional approaches [10]. Additionally, PV-wind-battery systems with multifunctional control techniques are being presented. These concepts examine energy flow in bidirectional converters of micro grids, taking into account the battery state of charge [11].

The objective of this contribution is to design and develop a micro grid combining wind energy, solar energy, and energy storage systems, with a focus on the use of renewable energy sources [12]. An energy management system is proposed to maintain power balance in the micro grid, providing configurable and flexible control for various load demand variations and energy consumption scenarios [13], as well as fluctuations in renewable energy sources [14].

The remainder of the document is structured as follows: Sections 2-3 elaborate on the overall system design, converter topologies, and control techniques. Section 4 introduces the system management algorithm. The obtained results are then

discussed in Section 5. Finally, the document concludes with Section 6.

2. SYSTEM DESCRIPTION

Energy management in hybrid systems combining wind, solar, and battery storage connected to micro-grids presents a complex challenge, particularly concerning the intermittent nature of renewable sources and the management of battery charging and discharging. Renewable energy sources, such as wind and solar, are characterized by significant variability due to changing weather conditions. This intermittency makes it difficult to match energy supply with real-time demand, potentially leading to periods of energy surplus or shortage. Additionally, effectively managing battery charge and discharge cycles to regulate energy supply and demand poses a major challenge for several reasons: precisely controlling battery charge levels to avoid overcharging or excessive discharge, balancing the load between renewable sources and battery storage considering high production periods and micro-grid energy needs, responding to demand variations, and ensuring optimal battery management to extend their lifespan while maintaining effective integration within the micro-grid.

In this study, the electricity production system under investigation primarily consists of a wind energy conversion system comprising a wind turbine (WT) utilizing a permanent magnet synchronous generator (PMSG), as well as a photovoltaic solar generator (GPV). Batteries are also present to store excess produced energy, playing a crucial role in maintaining the energy balance of the system. Additionally, the system is supplemented by static power converters and maximum power point tracking (MPPT) control. The entire system is connected to the electrical grid via a filter, as illustrated in Figure 1.

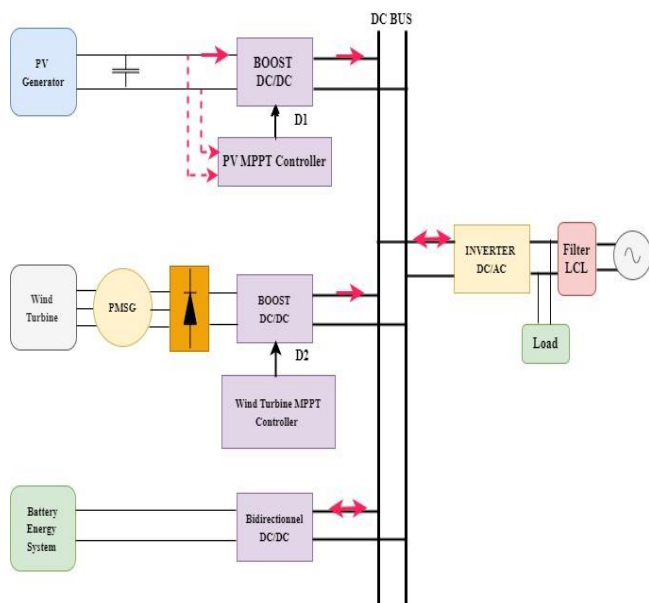


Figure 1. Proposed system hybrid storage scheme

The operation of this hybrid structure relies on utilizing the photovoltaic generator as the primary electricity production source, while the wind turbine and storage batteries serve as auxiliary sources to power the load. This load is consistently

and instantaneously connected to the electrical distribution grid, regardless of weather conditions and electricity demand requirements.

The system is designed to operate as follows, depending on various scenarios corresponding to inevitable climate changes:

- Under favorable solar and wind conditions:* When weather conditions are favorable, the photovoltaic solar generator (PV) produces electricity from solar energy, while the wind turbine generates electricity from the wind. This electricity is used to power the load connected to the electrical distribution grid. Any excess electricity produced is stored in the storage batteries for later use.
- Abundant sunshine, low wind:* In weather conditions where there is abundant sunshine but low wind, the solar PV generator becomes the main source of electricity to power the load. The storage batteries are used to compensate for the lack of electricity generated by the wind turbine.
- Abundant sunlight, weak wind:* In the event of weather conditions characterized by abundant sunlight but weak wind, the photovoltaic solar generator (PV) becomes the primary source of electricity to power the load. The storage batteries are utilized to compensate for the lack of electricity produced by the wind turbine.
- Extreme weather conditions:* In the event of extreme weather conditions where neither sufficient sunlight nor wind is available to produce electricity, the system can draw electricity from the electrical distribution grid to meet the load's needs. The storage batteries can also be utilized in emergency situations to ensure continuous power supply to the load.

3. MODELISATION

3.1 Solar energy conversion system

Photovoltaic cells, fundamental components of solar technology used in the production of solar panels and photovoltaic generators, convert light into electrical energy through the photovoltaic effect. They are typically arranged in series and parallel to form a solar panel. However, in specialized documentation, it is common to adopt a simplified electrical model, comprising a single diode (as illustrated in Figure 2), to represent a silicon photovoltaic cell and simulate its behavior. This model consists of a photocurrent source, a nonlinear diode, a series resistance reflecting internal losses, and a resistance connected in parallel with the diode to account for leakage current to the ground.

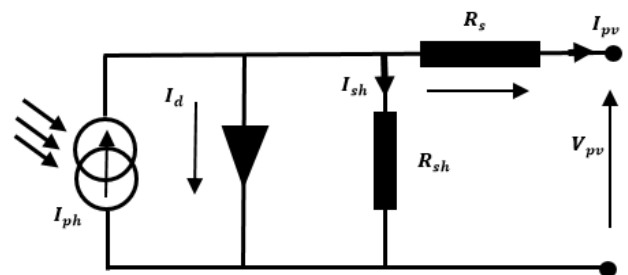


Figure 2. Electrical circuit equivalent of a GPV cell

From this circuit, these equations can be derived [15, 16]:

$$I_{pv} = I_{ph} - I_d - I_{sh} \quad (1)$$

The current flowing through these components is determined by the voltage applied across them.

$$V_d = V_{pv} + I_{pv} R_s \quad (2)$$

According to the Shockley diode equation, the current flowing through the diode can be expressed as:

$$I_d = I_0 \left[e^{\left(\frac{qV_d}{nkT} \right)} - 1 \right] \quad (3)$$

According to Ohm's Law, the current passing through the shunt resistor can be determined by dividing the voltage across the resistor by its resistance, as follows [17]:

$$I_{sh} = \frac{V_d}{R_{sh}} \quad (4)$$

$$I_{pv} = I_{ph} - I_0 \left[e^{\left(\frac{q(V_{pv} + I_{pv} R_s)}{nkT} \right)} - 1 \right] - \frac{V_{pv} + I_{pv} R_s}{R_{sh}} \quad (5)$$

where, I_{ph} : photocurrent; I_{pv} : cell output current; V_{pv} : cell's output voltage; V_d : voltage across diode; I_0 : reverse saturation current; R_{sh} : shunt resistance; R_s : serie resistance; N_s : number of cells in one module; n : diode ideality factor; k : Boltzmann's constant (1.381×10^{-23}); T : absolute temperature equals-273.15°C and q : electron charge (1.602×10^{-19} C).

Two solar panels are equipped with an adjustable irradiance constant by the user, with a default value set to 1000 W/m².

The described model was implemented using Matlab/Simulink software, taking into account the provided parameters outlined in Table 1.

Table 1. Parameters of the GPV

GPV's Characteristics	Value
Maximum power of panel Pmp	250 W
Cells per module Ncell	60
Open circuit voltage (Voc)	37.3 V
Short-circuit current (Isc)	8.66 A
Voltage at maximum power point (Vmp)	30.7 V
Parallel strings	1
Modules per string	8

Next, the system underwent testing across four levels of solar irradiation: 1000W/m² (standard), 800W/m², 600W/m², and 400W/m², with the temperature held constant at 25°C.

Figure 3 illustrates the current and power characteristic curves plotted against the voltage of the PV array, represented respectively by $I=f(V)$ and $P=f(V)$.

According to the characteristics $P=f(V)$ illustrated in Figure 3, it is observed that the maximum power that the photovoltaic generator can produce depends on the level of irradiation. Therefore, to ensure optimal operation at maximum power, the implementation of a control system is essential to monitor the maximum power point (MPP). Table 2 provides additional information on this subject.

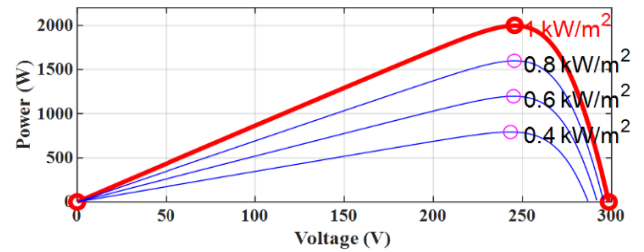
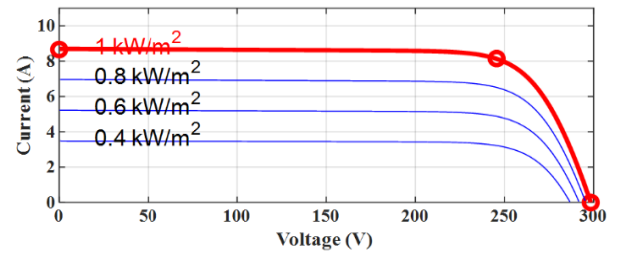


Figure 3. $I=f(V)$ and $P=f(V)$ of GPV for different irradiances

Table 2. Ppv_Max under different irradiations

Irradiation W/m ²	Ppv_Max (w)
400	736.15
600	1123.5
800	1516.6
1000	2e + 03

3.2 Wind energy conversion system

The Wind Energy Conversion System (WECS) consists of a wind turbine, a Permanent Magnet Synchronous Generator (PMSG), a DC-DC boost converter, and a controller. The extraction of power from the wind follows the description provided in reference [18]. Identify applicable funding agency here. If none, delete this text box.

$$P_w = 1/2 \rho A v^3 C_p(\lambda, \theta) \quad (6)$$

Here, ρ represents the air density in kg/m³, A denotes the area swept by the rotor blades in m², and v stands for the wind velocity in m/s. C_p , the power coefficient, is determined by the tip speed ratio (TSR) and pitch angle, represented by λ and θ , respectively, and are designed accordingly [19].

The different characteristics of the wind turbine's output power as a function of its speed for various wind speeds are shown in Figure 4 and the parametres of the wind system used in this work is shown in Table 3.

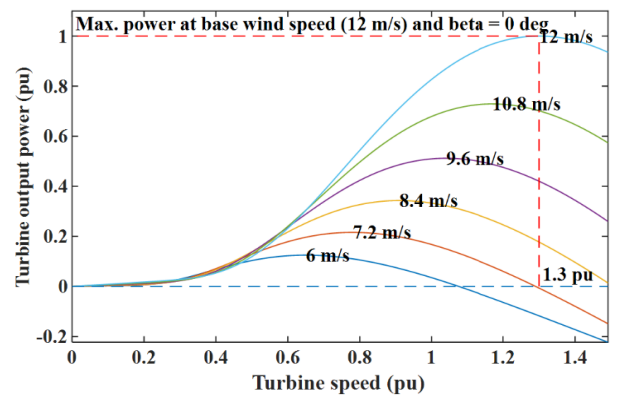


Figure 4. Wind turbine mechanical characteristics across varying wind speeds

Table 3. Parameters of WECS

Parameters	Value
Maximum power	3 KW
Wind	12 m/s
Wind turbine radius (R)	5 m
Wind density (ρ)	1.22 kg/m ²
Maximum range	25 m/s

3.3 Modeling of PMSG

The widely employed mathematical model of the Permanent Magnet Synchronous Generator (PMSG) in the rotor reference dq frame is depicted as follows:

$$\begin{cases} V_{sd} = R_g i_d - \omega_e \varphi_{sq} + \frac{d\varphi_{sd}}{dt} \\ V_{sq} = R_g i_q - \omega_e \varphi_{sd} + \frac{d\varphi_{sq}}{dt} \end{cases} \quad (7)$$

where, V_{sd} and V_{sq} denote the stator voltage, i_d and i_q signify the stator current, φ_{sd} and φ_{sq} denote the stator flux in frames [20]. R_g represents the stator resistance, while ω_e denotes the electrical rotation speed of the PMSG, defined as follows [21]:

$$\omega_e = p_r \omega_{rm} \quad (8)$$

where, p_r : is the number of pole pairs.

The stator flux expressions are as follows:

$$\begin{cases} \varphi_{sd} = L_d i_d + \varphi_f \\ \varphi_{sq} = L_q i_q \end{cases} \quad (9)$$

where, L_d and L_q represent the generator inductances on the d and q axes, respectively, and φ_f the permanent magnetic flux.

The expression for the electromagnetic torque is as follows:

$$T_e = \frac{3}{2} p_r (\varphi_{sd} i_q - \varphi_{sq} i_d) \quad (10)$$

By substituting Eq. (7) into Eq. (9), the model of the Permanent Magnet Synchronous Generator (PMSG) in the synchronous reference frame can be expressed as follows:

$$\begin{cases} V_{sd} = R_g i_d + L_d \frac{di_d}{dt} - L_q i_q \omega_e \\ V_{sq} = R_g i_q + L_q \frac{di_q}{dt} + L_d i_d \omega_e + \omega_e \varphi_f \end{cases} \quad (11)$$

The electromagnetic torque in Eq. (10) is rewritten as follows:

$$T_e = \frac{3}{2} p_r [\varphi_f i_q + (L_d - L_q) i_d i_q] \quad (12)$$

Assuming equal inductances on the d and q axes for the PMSG (L_d / L_q), the expression for the electromagnetic torque in Eq. (12) can be described as follows [22]:

$$T_e = \frac{3}{2} p_r i_q \varphi_f \quad (13)$$

The parameters system is shown in Table 4.

Table 4. Parameters of filter and inverter

Parameters	Value
DC bus	400 V
Grid voltage	230 V
Grid frequency	50 HZ
Switching frequency	20 KVA
Grid-filter inductance	10e-3 pu
Inductor Lin	4.06 mH
Geid filter capacitor	6.017 uF
Controller time constant	150 us

3.4 Modeling of battery system

The choice of solar battery type is crucial due to its use in multi-source systems. They are categorized into three distinct types based on their technology: maintenance-free batteries, with an efficiency of around 80%; lead-acid batteries, with an efficiency of around 90%; and lithium-ion batteries, the most efficient, with an efficiency of around 98% [23-25]. The use of lithium-ion batteries in multi-source energy management systems is justified by several key factors that meet the specific requirements of these systems. Compared to lead-acid or nickel-cadmium batteries, lithium-ion batteries offer a higher energy density, making them suitable for energy storage applications where long-term reliability is necessary. They also exhibit low energy loss during storage and discharge processes and can respond quickly to charging and discharging needs. Furthermore, lithium-ion batteries are generally lighter and more compact than other types of batteries.

Modeling a lithium-ion battery is intricate, encompassing the consideration of numerous parameters including battery capacity, internal resistance, voltage, temperature, and charge/discharge rate. Mathematical models such as the equivalent circuit model are frequently employed to characterize these batteries and forecast their performance under varying usage scenarios. In this study, Figure 5 illustrates the equivalent electrical circuit of the battery utilized, while Eqs. (14) and (15) represent the battery voltage (V_{Bat}) and state of charge (SOC) [26, 27].

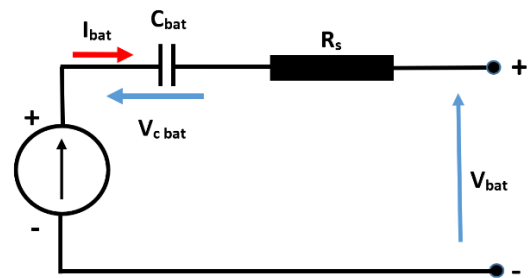


Figure 5. RC model of the battery

$$V_{Bat} = E_0 - R_{Bat} I_{Bat} - k \cdot \int \frac{I_{Bat}}{Q} dt \quad (14)$$

$$SOC = 100 \left(1 + \frac{\int I_{bat} dt}{Q} \right) \quad (15)$$

where, Q is the battery capacity and I_{Bat} denotes the battery current, which operates in: charging and discharging modes,

depending on the power generated by solar and wind energy [28]. The battery parameters are defined in Table 5.

Table 5. Parameters of battery

Parameters	Value
Nominal voltage	12×20 V
Rated capacity	48 Ah
Initial Soc	9%
Battery response time	0.0001

The battery also operates in these two modes based on the energy constraints dictated by the state of charge (SOC) limits, as determined by [29].

$$SOC_{min} \leq SOC \leq SOC_{max} \quad (16)$$

4. INTELLIGENT POWER MANAGEMENT CONTROL

The method for managing standalone hybrid systems is designed to meet charging demands and control power flow, thus ensuring efficient operation of all energy sources. The power balance equation is formulated as follows:

$$P_w + P_{pv} = P_L + P_{bat} \quad (17)$$

The energy management system functions across four distinct modes, each contingent upon two main parameters: energy production and battery charge level.

The preferred operating mode occurs when the power generated by the Solar Energy Conversion System (SECS) and the Wind Energy Conversion System (WECS) exceeds the load demand. At this point, the battery is charged until it reaches the maximum state of charge level (SOC_{max}). Once the battery's SOC reaches SOC_{max} , the Maximum Power Point Tracking (MPPT) controller is deactivated, and the battery stops being recharged [30]. When the MPPT controller is disabled, solar energy production decreases as the total production exceeds the demand, and the surplus energy cannot be used to charge the battery anymore. At this point, the battery fully supplies the load requirements [31].

However, in the event of insufficient production from solar and wind sources to meet the demand, the battery compensates for the power deficit. This process continues until the SOC reaches SOC_{min} [32]. Once this threshold is reached, shedding becomes necessary to maintain electrical balance, as the electricity supply falls below demand.

4.1 Fuzzy energy management architecture

The application of fuzzy logic significantly enhances the overall performance and efficiency of the system by enabling effective coordination and management of energy distribution. Fuzzy Systems (FS) are based on the theory of fuzzy sets, employing a nonlinear control approach aimed at applying the knowledge of an experienced user to design a fuzzy logic-based controller [33]: Fuzzification, Fuzzy rule evaluation (fuzzy inference engine), and Defuzzification.

The system management strategy must determine how to distribute power among energy sources such as photovoltaic, wind, grid, and battery while ensuring the satisfaction of the load's energy needs. Given the inherent uncertainty in

electricity demand, subject to frequent variations, establishing a load profile becomes inevitable. This complexity is exacerbated by the presence of nonlinear subsystems within the hybrid system. Therefore, it is relevant to consider a fuzzy anticipation of both demand and state of charge (SOC).

Figure 6 illustrates the proposed fuzzy expert system, specifically designed to adapt to weather fluctuations, load variations, and energy consumption. Figure 7 shows the membership functions for the battery state generated power, load power and battery state.

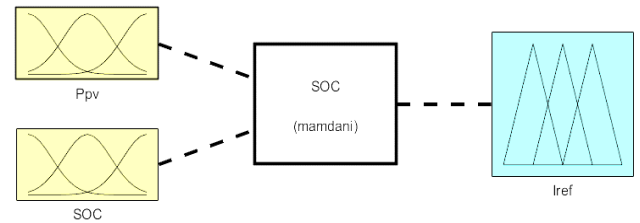


Figure 6. Fuzzy expert system

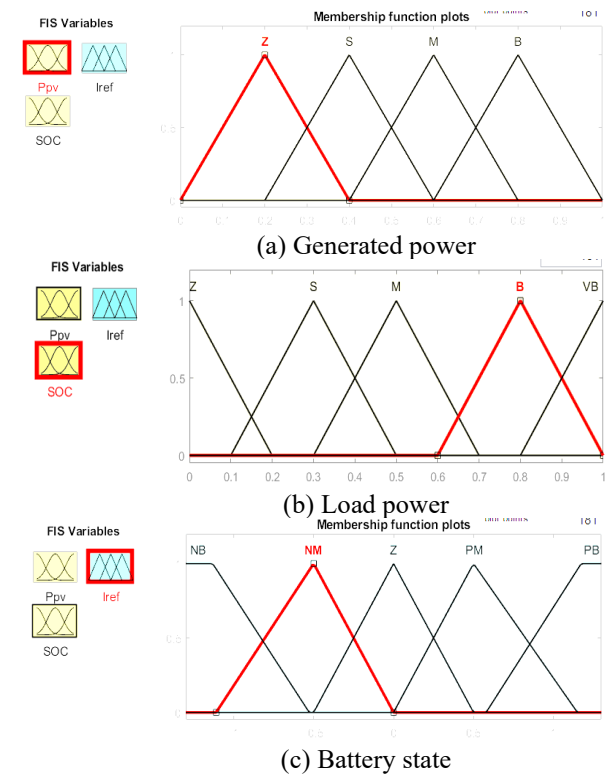


Figure 7. Membership functions of the FLC

Table 6. Fuzzy logic rules

SOC/P	Z	S	M	B
Z	NB	NB	NM	NM
S	NB	NB	NM	NM
M	NM	NM	PM	PM
B	PB	PM	PB	PB
VB	PB	PB	PB	PB

In typical operational scenarios, the system's power undergoes a gradual evolution to minimize deviation from the grid's operational point [34]. The battery management system is responsible for maintaining the battery's state of charge at an optimal level, usually around 50%. Furthermore, it assumes a pivotal role in mitigating voltage drops by regulating the

necessary power level of the battery. This meticulous control mechanism guarantees the battery's sustained operability and its ability to furnish consistent power, consequently bolstering the overall stability of the energy system [35]. Table 6 shows the fuzzy rules applied in the controller.

5. RESULTS AND SIMULATION

Figure 8 presents the profiles of wind speed and solar irradiance used for simulation tests aimed at analyzing and evaluating the performance of the management system adopted in various environmental scenarios.

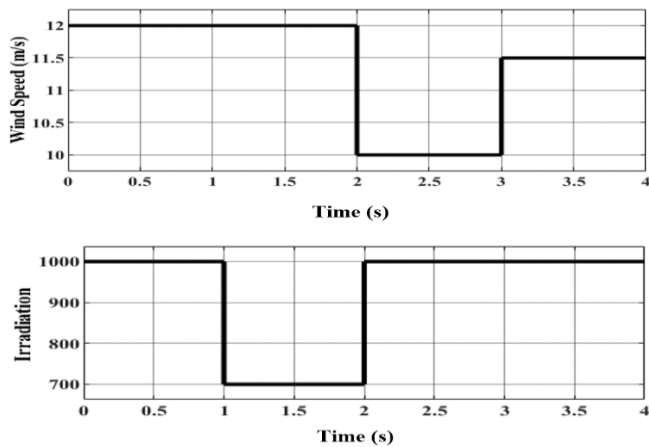


Figure 8. Profiles of wind speed and solar irradiance levels

We subjected the system to two different profiles and numerically simulated its behavior for two load scenarios. In the first case, the load power is kept constant, while in the second case, it varies. The analysis of the system's behavior under these conditions is presented below:

Case 1. Fixed load power

Figures 9 and 10 illustrate, respectively, the evolution of the load power (Pload) and that produced by the renewable energy sources (RES), notably those from the photovoltaic generator (Ppv) and the wind turbine (Pw) and the evolution of state of charge of battery for constant load.

For such an operating scenario, there are primarily four (4) distinct time intervals during which the batteries alternate between two (2) intervals in charging mode and the other two in discharging mode, as explained below. So, for each time interval, we observe that:

From 0 to 1s: The temporal analysis of the power (see Figure 9) shows that the power levels evolve rapidly (response time of approximately 0.001s) to reach the levels corresponding to the weather conditions (irradiation and wind speed) shown in Figures 3 and 4 within this time frame. The power from the renewable energy sources (RES) is 4500 W, which exceeds the load demand of 3500 W. This excess power is used to charge the battery, increasing the SOC to 50.0007%, as shown in Figure 10.

From 1s to 2s: During this time interval, the power demanded by the load remains at 3500 W, while the sum of the powers produced by the renewable energy sources (RES) is approximately 3400 W. Therefore, to meet the load power demand, the missing power of 100 W is provided by the batteries, resulting in a decrease in SOC from 50.0007% to 50.0006%, as shown in Figure 10 during the period from 1 second to 2 seconds.

From 2s to 3s: The sum of the powers produced by the RES is 2900 W, which is less than the load demand of 3500 W. Therefore, the batteries continue to discharge, (battery discharge mode, "Decrease in SOC to 50.0006%") approximately 49.998% to provide the missing power 600 W.

From 3s to 4s: For this last time interval, it is observed from Figure 9 that the sum of the powers produced by the RES is equal to 4100 W, which is greater than the one required for the load. Consequently, the batteries transition from the discharge mode to the charge mode ("Increase in SOC from 49.998% to 49.9985%"), as shown in Figure 10.

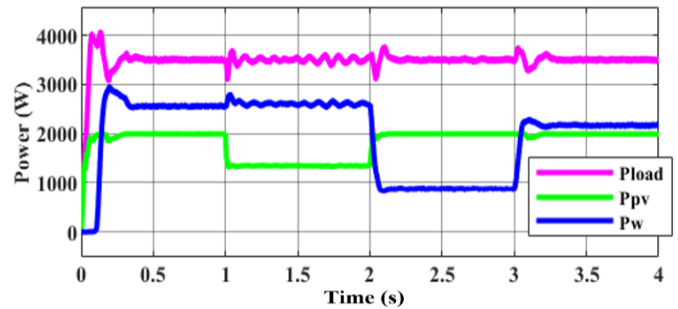


Figure 9. Power at different locations for constant load

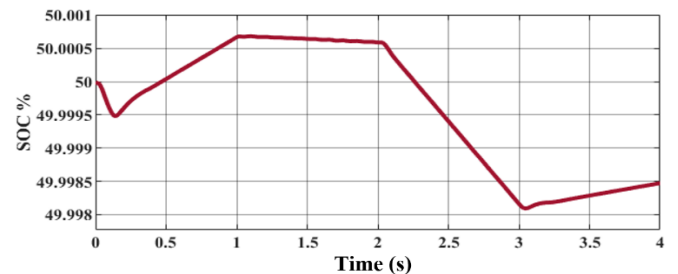


Figure 10. State of charge of battery for constant load

Case 2. Variable load power

In the case where the load power varies, as illustrated in Figure 11, and under the same conditions of irradiation and wind change previously considered, Figures 11 and 12 respectively depict the powers and the state of charge of the batteries (SOC).

Based on the two preceding figures, the following observations can be made for the four time intervals:

From 0 to 1s: During this time interval, the load power is 1000 W, while the sum of the powers produced by the RES is equal to 4600 W, which is sufficient to meet the load power requirements. The excess power is then stored in the batteries. This is justified by the increase in SOC observed in Figure 12.

From 1s to 2s: In this time interval, there is a decrease in irradiation level, while the wind speed and load power remain unchanged compared to the previous interval. Thus, the sum of the powers produced by the RES is approximately 3900 W, which is sufficient to meet the load demand and provide the excess to the batteries, which continue to charge as shown in Figure 12.

From 2s to 3s: During this interval, the load power has increased to 2900 W, due to the weather changes, the sum of the RES powers corresponding to this environment is 2800 W. Therefore, the lack of power to satisfy the load demand is compensated by transitioning from the battery charging mode to discharge mode, resulting in a decrease in SOC.

From 3s to 4s: The load power demanded is 3200 W, while

the sum of the powers produced by the RES is 4200 W, resulting in an excess of power. The batteries are thus operating in charge mode, justified by the increase in SOC in Figure 12.

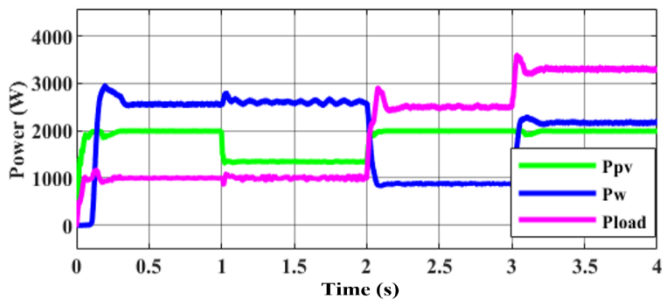


Figure 11. Power at different locations for variable load

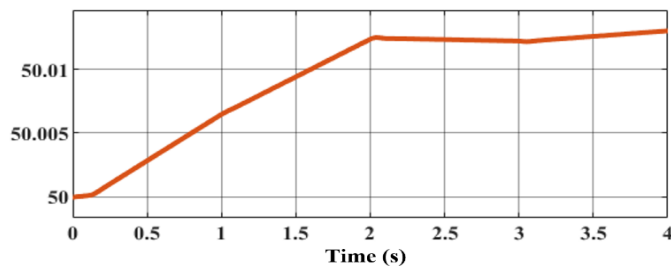


Figure 12. State of charge of battery for variable load

However, following this analysis of the different scenarios close to reality, it is proven that the system operates correctly according to the specifications. The analysis of SOC variations is crucial for the battery's lifespan and the overall performance of the hybrid system. Indeed, proper SOC management is essential to ensure optimal performance and extend the battery's life. In terms of energy efficiency, the SOC is generally maintained within an optimal range between 20% and 80%, which we have adopted as a condition for our simulations. It is important to note that an SOC that is too high (Soc=100%) or too low (SOC=0%) can accelerate the chemical degradation of battery cells. However, based on the analysis specific to each previously discussed time interval, we observe that the SOC varies between 49.998% and 50.001% for Case 1: Fixed load power (see Figure10) and 50 % to 50, 0013 %) for Case 2: Variable load power. Consequently, it is properly maintained within the defined range, thereby prolonging the battery life. Additionally, the temporal power analysis shows, for both cases, that the response time is quick and sufficient to provide energy instantly to reach the optimal power level during fluctuations in energy demand, thus ensuring the stability of the electrical grid.

6. CONCLUSIONS

This paper explores intelligent energy management control for hybrid systems combining wind, solar, and battery technologies, based on fuzzy logic. The study demonstrated that this approach optimizes energy resource management, especially in contexts where renewable energy sources exhibit significant intermittency and variability.

The fuzzy logic control has proven its effectiveness by providing more precise and adaptable energy flow management, thanks to the increased responsiveness of the

hybrid system to variations in weather conditions. The importance of maintaining the state of charge (SOC) of batteries within an optimal range to extend their lifespan and ensure stable system performance has also been highlighted. Dynamic SOC management has thus enabled more effective balancing of energy production and demand. However, while fuzzy logic improves energy management, the approach can become complex to implement and adjust, especially with an increasing number of energy sources or batteries. This may require additional resources to maintain control efficiency.

This work underscores the crucial importance of effective integration of renewable energies into the electrical grid to support the transition to a cleaner and more resilient energy future. Looking ahead, it would be interesting to explore in future research the integration of fuzzy logic with artificial intelligence techniques, such as machine learning, to further enhance the dynamic and predictive management of hybrid systems.

REFERENCES

- [1] Aliyu, A.K., Modu, B., Tan, C.W. (2018). A review of renewable energy development in Africa: A focus in South Africa, Egypt and Nigeria. *Renewable and Sustainable Energy Reviews*, 81: 2502-2518. <https://doi.org/10.1016/j.rser.2017.06.055>
- [2] Belfedhal, S.A., Berkouk, E.L., Messlem, Y. (2019). Analysis of grid connected hybrid renewable energy system. *Journal of Renewable and Sustainable Energy*, 11(1): 014702. <https://doi.org/10.1063/1.5054869>
- [3] Nehrir, M.H., Wang, C., Strunz, K., Aki, H., Ramakumar, R., Bing, J., Miao, Z., Salameh, Z. (2011). A review of hybrid renewable/alternative energy systems for electric power generation: Configurations, control, and applications. *IEEE Transactions on Sustainable Energy*, 2(4): 392-403. <https://doi.org/10.1109/TSTE.2011.2157540>
- [4] Arsad, A.Z., Hannan, M.A., Al-Shetwi, A.Q., Mansur, M., Muttaqi, K.M., Dong, Z.Y., Blaabjerg, F. (2022). Hydrogen energy storage integrated hybrid renewable energy systems: A review analysis for future research directions. *International Journal of Hydrogen Energy*, 47(39): 17285-17312. <https://doi.org/10.1016/j.ijhydene.2022.03.208>
- [5] Khan, A.A., Minai, A.F., Pachauri, R.K., Malik, H. (2022). Optimal sizing, control, and management strategies for hybrid renewable energy systems: A comprehensive review. *Energies*, 15(17): 6249. <https://doi.org/10.3390/en15176249>
- [6] Ren, G., Wang, J., Li, Y., Zhang, G. (2023). Power distribution optimization of a fully active hybrid energy storage system configuration for vehicular applications. *Journal of Industrial Information Integration*, 33: 100459. <https://doi.org/10.1016/j.jii.2023.100459>
- [7] Shafiullah, G.M., Masola, T., Samu, R., Elavarasan, R.M., Begum, S., Subramaniam, U., Romlie, M.F., Chowdhury, M., Arif, M.T. (2021). Prospects of hybrid renewable energy-based power system: A case study, post analysis of Chipendeke Micro-Hydro, Zimbabwe. *IEEEAccess*, 9: 73433-73452. <https://doi.org/10.1109/ACCESS.2021.3078713>
- [8] Awan, M.M.A., Javed, M.Y., Asghar, A.B., Ejsmont, K. (2022). Economic integration of renewable and

- conventional power sources—A case study. *Energies*, 15(6): 2141. <https://doi.org/10.3390/en15062141>
- [9] Krishnan, M.S., Ramkumar, M.S., Amudha, A. (2017). Frequency deviation control in hybrid renewable energy system using FC-UC. *International Journal of Control Theory and Applications*, 10(2): 333-344. https://serialsjournals.com/abstract/27407_37--cha-48.
- [10] Ibrahim, A.M.A., Nourelddeen, O. (2018). Performance analysis of grid connected pv/wind hybrid power system during variations of environmental conditions and load. *International Journal of Renewable Energy Research*, 8(1): 208-220. <https://doi.org/10.20508/ijrer.v8i1.6702.g7347>
- [11] Jamali, A.A., Nor, N.M., Ibrahim, T. (2015). Energy storage systems and their sizing techniques in power system—A review. In 2015 IEEE Conference on Energy Conversion, Johor Bahru, Malaysia, pp. 215-220. <https://doi.org/10.1109/CENCON.2015.7409542>
- [12] Oskouei, A.B., Banaei, M.R., Sabahi, M. (2016). Hybrid PV/wind system with quinary asymmetric inverter without increasing DC-link number. *Ain Shams Engineering Journal*, 7(2): 579-592. <https://doi.org/10.1016/j.asej.2015.06.008>
- [13] Belabbas, B., Allaoui, T., Tadjine, M., Denai, M. (2017). Power quality enhancement in hybrid photovoltaic-battery system based on three-level inverter associated with DC bus voltage control. *Journal of Power Technologies*, 97(4): 272-282. <http://papers.itc.pw.edu.pl/index.php/JPT/article/view/992>.
- [14] Das, S., Akella, A.K. (2018). Power flow control of PV-wind-battery hybrid renewable energy systems for stand-alone application. *International Journal of Renewable Energy Research (IJRER)*, 8(1): 36-43. <https://doi.org/10.20508/ijrer.v8i1.6534.g7278>
- [15] Pachanapan, P., Apichayaku, P., Vongkunghae, A., Tantanee, S. (2022). Islanding operation among solar hybrid system and grid-tied PV system in buildings. *International Energy Journal*, 22(1): 25-34. <http://www.ericjournal.ait.ac.th/index.php/eric/article/view/2836/pdf>.
- [16] Bouziane, Y.S., Henini, N., Tlemçani, A. (2022). Energy management of a hybrid generation system based on wind turbine coupled with a battery/supercapacitor. *Journal Européen des Systèmes Automatisés*, 55(5): 623-631. <https://doi.org/10.18280/jesa.550507>
- [17] Patel, M., Bohra, S. (2023). Power management of grid-connected PV wind hybrid system incorporated with energy storage system. *Future Energy*, 2(1): 7-19. <https://doi.org/10.55670/fpll.fuen.2.3.2>
- [18] Abo-Khalil, A.G., Eltamaly, A.M., RP, P., Alghamdi, A. S., Tlili, I. (2020). A sensorless wind speed and rotor position control of PMSG in wind power generation systems. *Sustainability*, 12(20): 8481. <https://doi.org/10.3390/su12208481>
- [19] Priyadarshi, N., Sharma, A.K., Azam, F. (2017). A hybrid firefly-asymmetrical fuzzy logic controller based MPPT for PV-wind-fuel grid integration. *International Journal of Renewable Energy Research*, 7(4): 1546-1560. <https://doi.org/10.20508/ijrer.v7i4.6131.g7195>
- [20] Mazare, M., Taghizadeh, M., Ghaf-Ghanbari, P. (2021). Pitch actuator fault-tolerant control of wind turbines based on time delay control and disturbance observer. *Ocean Engineering*, 238: 109724. <https://doi.org/10.1016/j.oceaneng.2021.109724>
- [21] Jiang, Z. (2021). Installation of offshore wind turbines: A technical review. *Renewable & Sustainable Energy Reviews*, 139: 110576. <https://doi.org/10.1016/j.rser.2020.110576>
- [22] Mousa, H.H., Youssef, A.R., Mohamed, E.E. (2019). Variable step size P&O MPPT algorithm for optimal power extraction of multi-phase PMSG based wind generation system. *International Journal of Electrical Power & Energy Systems*, 108: 218-231. <https://doi.org/10.1016/j.ijepes.2018.12.044>
- [23] Moe, K.M., Ya, A.Z., Aung, N.W. (2019). Performance comparison for different MPPT methods used with stand-alone PV system. *Journal of Science, Engineering and Technology Research*, 1(1): 129-134.
- [24] Hussain Nengroo, S., Umair Ali, M., Zafar, A., Hussain, S., Murtaza, T., Junaid Alvi, M., Raghavendra, K.V.G., Jee Kim, H. (2019). An optimized methodology for a hybrid photo-voltaic and energy storage system connected to a low-voltage grid. *Electronics*, 8(2): 176. <https://doi.org/10.3390/electronics8020176>
- [25] Jadhav, S., Devdas, N., Nisar, S., Bajpai, V. (2018). Bidirectional DC-DC converter in solar PV system for battery charging application. In 2018 International Conference on Smart City and Emerging Technology (ICSCET), Mumbai, India, pp. 1-4. <https://doi.org/10.1109/ICSCET.2018.8537391>
- [26] Nguyen, H.T., Al-Sumaiti, A.S., Vu, V.P., Al-Durra, A., Do, T.D. (2020). Optimal power tracking of PMSG based wind energy conversion systems by constrained direct control with fast convergence rates. *International Journal of Electrical Power & Energy Systems*, 118: 105807. <https://doi.org/10.1016/j.ijepes.2019.105807>
- [27] Benmouna, A., Becherif, M., Boulon, L., Dépature, C., Ramadan, H.S. (2021). Efficient experimental energy management operating for FC/battery/SC vehicles via hybrid artificial neural networks-passivity based control. *Renewable Energy*, 178: 1291-1302. <https://doi.org/10.1016/j.renene.2021.06.038>
- [28] León Gómez, J.C., De León Aldaco, S.E., Aguayo Alquicira, J. (2023). A review of hybrid renewable energy systems: Architectures, battery systems, and optimization techniques. *Eng*, 4(2): 1446-1467. <https://doi.org/10.3390/eng4020084>
- [29] Pattnaik, S., Kumar, M.R., Mishra, S.K., Gautam, S.P., Appasani, B., Ustun, T.S. (2022). DC bus voltage stabilization and SOC management using optimal tuning of controllers for supercapacitor based PV hybrid energy storage system. *Batteries*, 8(10): 186. <https://doi.org/10.3390/batteries8100186>
- [30] Li, R., Shi, F. (2019). Control and optimization of residential photovoltaic power generation system with high efficiency isolated bidirectional DC-DC converter. *IEEE Access*, 7: 116107-116122. <https://doi.org/10.1109/ACCESS.2019.2935344>
- [31] Alnejaili, T., Drid, S., Mehdi, D., Chrifi-Alaoui, L., Belarbi, R., Hamdouni, A. (2015). Dynamic control and advanced load management of a stand-alone hybrid renewable power system for remote housing. *Energy Conversion and Management*, 105: 377-392. <https://doi.org/10.1016/j.enconman.2015.07.080>
- [32] Sarda, J.S., Lee, K., Patel, H., Patel, N., Patel, D. (2022). Energy management system of microgrid using optimization approach. *IFAC-PapersOnLine*, 55(9): 280-

284. <https://doi.org/10.1016/j.ifacol.2022.07.049>
- [33] Koulali, M., Mankour, M., Negadi, K., Mezouar, A. (2019). Energy management of hybrid power system PV Wind and battery based three level converter. *TECNICA ITALIANA-Italian Journal of Engineering Science*, 63(2-4): 297-304.
- [34] Roumila, Z., Rekioua, D., Rekioua, T. (2017). Energy management based fuzzy logic controller of hybrid system wind/photovoltaic/diesel with storage battery. *International Journal of Hydrogen Energy*, 42(30): 19525-19535. <https://doi.org/10.1016/j.ijhydene.2017.06.006>
- [35] Kumari, N., Aryan, P., Raja, G.L., Arya, Y. (2023). Dual degree branched type-2 fuzzy controller optimized with a hybrid algorithm for frequency regulation in a triple-area power system integrated with renewable sources. *Protection and Control of Modern Power Systems*, 8(3): 1-29. <https://doi.org/10.1186/s41601-023-00317-7>